PNAS NEXUS

PNAS Nexus, 2025, 4, pgaf100
https://doi.org/10.1093/pnasnexus/pgaf100
Advance access publication 27 March 2025
Research Report

Polychlorinated biphenyls induce immunometabolic switch of antiinflammatory macrophages toward an inflammatory phenotype

Riley M. Behan-Bush [a,b], Michael V. Schrodt [a,b], Elizabeth Kilburg [a], Jesse N. Liszewski [a,b], Laura M. Bitterlich [c,d], Karen English [c,d], Aloysius J. Klingelhutz [b,e] and James A. Ankrum [a,b,*]

[a]Roy J. Carver Department of Biomedical Engineering, University of Iowa, Iowa City, IA 52242, USA
[b]Fraternal Order of Eagles Diabetes Research Center, University of Iowa, Iowa City, IA 52242, USA
[c]Kathleen Lonsdale Institute for Human Health Research, Maynooth University, Maynooth, Ireland W23 F2H6
[d]Department of Biology, Maynooth University, Maynooth, Ireland W23 F2H6
[e]Department of Microbiology and Immunology, University of Iowa, Iowa City, IA 52242, USA
*To whom correspondence should be addressed: Email: james-ankrum@uiowa.edu
Guest Editor Robert Tukey
Accepted by Editor David Brenner

Abstract

Polychlorinated biphenyls (PCBs) are a group of environmental toxicants associated with increased risk of diabetes, obesity, and metabolic syndrome. These metabolic disorders are characterized by systemic and local inflammation within adipose tissue, the primary site of PCB accumulation. These inflammatory changes arise when resident adipose tissue macrophages undergo phenotypic plasticity—switching from an antiinflammatory to an inflammatory phenotype. Thus, we sought to assess whether PCB exposure drives macrophage phenotypic switching. We investigated how human monocyte-derived macrophages polarized toward an M1, M2a, or M2c phenotype were impacted by exposure to Aroclor 1254, a PCB mixture found at high levels in school air. We showed that PCB exposure not only exacerbates the inflammatory phenotype of M1 macrophages but also shifts both M2a and M2c cells toward a more inflammatory phototype in both a dose- and time-dependent manner. Additionally, we show that PCB exposure leads to significant metabolic changes. M2 macrophages exposed to PCBs exhibit increased reliance on aerobic glycolysis and reduced capacity for fatty acid and amino acid oxidation—both indicators of an inflammatory macrophage phenotype. Collectively, these results demonstrate that PCBs promote immunometabolic macrophage plasticity toward a more M1-like phenotype, thereby suggesting that PCBs exacerbate metabolic diseases by altering the inflammatory environment in adipose tissue.

Keywords: PCBs, immunometabolism, toxicology, plasticity

Significance Statement

Human exposure to the persistent organic pollutant, polychlorinated biphenyls (PCBs), has been linked to an increased risk of metabolic diseases such as diabetes and obesity. A key feature of these diseases is chronic inflammation, which often starts in adipose tissue when resident macrophages shift from an antiinflammatory to a proinflammatory state. Our study demonstrates that PCBs induce this shift by transforming antiinflammatory macrophages into a more inflammatory phenotype. Additionally, we found that this phenotypic change is associated with altered cellular metabolism, as PCB-exposed macrophages exhibit increased reliance on glycolysis and glucose metabolism. These findings suggest that PCBs contribute to the pathogenesis of metabolic disease by altering the immunometabolic state of adipose tissue.

Introduction

Polychlorinated biphenyls (PCBs) are a group of environmental toxicants that were produced in large quantities before manufacturing was banned in 1979. There are 209 distinct PCB congeners; however, they were not produced in their single congener state but rather as mixtures of 50–80 congeners. These mixtures, sold under the tradename "Aroclor," were and continue to be the primary source of PCB exposure (1). Despite production being banned for 50 years, Aroclors produced before 1979 are still found at high levels in the environment and in building materials such as capacitors, transformers, caulk, paint, and more making PCBs ubiquitous in public spaces (2–5). Exacerbating the problem is the

Competing Interest: The authors declare no competing interests.
Received: October 7, 2024. **Accepted:** February 28, 2025

fact that the PCB congeners found in Aroclors, particularly lower chlorinated congeners, are volatile, making inhalation a major route of toxicant exposure (1, 6–8). Consequently, significant amounts of PCBs, particularly signatures of Aroclor 1254, can still be measured in school air today (7–11). Research by our colleagues in the Iowa Superfund Research Program (ISRP) has shown that indoor school air can have up to 100 × higher concentrations of PCBs than air measured outdoors near Superfund sites, and children and teachers attending these schools have higher serum levels of PCBs compared with those in noncontaminated schools (8, 9). Thus, there is a significant need to understand how exposure to Aroclor 1254 affects human health and development.

Human exposure to PCBs has been linked to an increased risk of heart disease, cancer, and the development of metabolic syndrome that includes obesity, hyperlipidemia, and type II diabetes (12–15). However, the mechanisms by which PCBs cause these diseases are not well understood. Metabolic syndrome is characterized by insulin resistance, dyslipidemia, increased adiposity, as well as systemic and local inflammation (16). Adipose tissue, which helps regulate metabolism and insulin sensitivity, is central to the development of metabolic syndrome (17). Adipose tissue is also of particular importance for understanding the impact of PCBs on human health because PCBs are lipophilic and accumulate in lipid-rich adipocytes, the primary cells in adipose tissue (18–20). Therefore, most research to date has focused on understanding how PCBs impact adipocytes and their precursors, adipose mesenchymal stem cells. This research has shown that PCBs interfere with adipocyte differentiation, alter adipokine secretion, and activate inflammatory gene pathways (21–23). However, since adipose tissue consists of more than just adipocyte lineage cells, this work has only partially addressed how PCBs could be contributing to metabolic syndrome. Although PCBs have direct effects on adipocytes and adipocyte precursors, they could also exert indirect effects on adipose health by impacting tissue-resident immune cells to cause or propagate adipose tissue inflammation (24).

Adipose tissue inflammation is initiated by resident macrophages. While macrophages are often discussed in terms of inflammatory (M1) vs. antiinflammatory (M2) phenotypes, a strict M1/M2 dichotomy does not exist in vivo. Instead, macrophages slide along the spectrum toward a more inflammatory or antiinflammatory phenotype depending on external stimuli. In healthy adipose, macrophages work in harmony with adipocytes to regulate metabolism and insulin sensitivity by adopting an antiinflammatory, M2-like phenotype (25). These M2 macrophages can be further subdivided into M2a, M2b, and M2c, which each play a distinct role in maintaining adipose homeostasis (26–28). However, macrophages have an incredible capacity to alter their phenotype in response to their surrounding environment. Thus, in response to obesogenic stimuli, the resident antiinflammatory macrophages can be reprogrammed toward an inflammatory, M1-like state in a process known as macrophage plasticity. These inflammatory macrophages further promote adipocyte dysfunction by altering adipokine signaling, increasing insulin resistance, and driving adipocyte hypertrophy (29). Furthermore, these macrophages release inflammatory cytokines and chemokines that promote additional phenotype switching and recruit monocytes to adipose tissue where they differentiate into new macrophages (30). What starts as a small switch in macrophage phenotype can lead to a self-propagating cycle of adipose tissue inflammation that stimulates systemic inflammation and exacerbates metabolic disease (31, 32).

Despite the essential role macrophages play in adipose tissue health and disease, little is known about how PCBs impact macrophages. Most animal studies have focused on how PCB exposure impacts systemic inflammatory markers. For example, Zhang et al. (33) showed that Aroclor 1254 increased the level of systemic inflammatory cytokines, interleukin 6 (IL-6) and tumor necrosis factor (TNF), and Petriello et al. (34) showed that mice exposed to PCB 126 had increased circulating monocytes, macrophages, and neutrophils. Others have shown that this systemic inflammation is accompanied by signs of adipose tissue inflammation including increased mRNA expression of inflammatory cytokines, *TNF*, *IL6*, *MCP1*, and *IL8* (35–38). Furthermore, a couple of research groups have shown the amount of toxicant accumulation in adipose directly correlates to the number of macrophages in the tissue (38, 39). However, despite these indications that the immunological state of adipose tissue is impacted by PCB exposure, how PCBs directly impact macrophages is not well understood. What we know to date comes from studies that have utilized macrophage cell lines and individual PCB congeners. Using the THP-1 macrophage cell line, for example, Wang et al. (40) and May et al. (41) showed that naïve macrophages exposed to PCB 126 or PCB 118 become inflammatory. In contrast, Santoro et al. (42) showed that naïve J77A.1 macrophages exposed to PCB 101, 153, or 180 exhibited reduced ability to respond to inflammatory stimuli. The use of THP-1 and J77A.1 cells complicates our ability to translate these findings to human disease since macrophage cell lines often respond differently to stimuli compared with primary human cells (43, 44). Furthermore, humans are rarely exposed to individual PCB congeners but are routinely exposed to complex mixtures of PCBs, since PCBs were originally manufactured as mixtures such as Aroclor 1254. Therefore, human samples such as adipose tissue contain not just one congener but a vast array of congeners (7, 45, 46). Consequently, there is a need to understand how exposure to PCB mixtures impacts human macrophages.

In this study, we sought to understand how exposure to environmentally relevant PCBs impacts the phenotypic profile of primary human monocyte-derived macrophages. Since humans are predominantly exposed to PCB mixtures, not single congeners, we chose to assess the impact of Aroclor 1254, a PCB mixture commonly found at high levels in school buildings built before 1980 (10). Because macrophages found in adipose tissue are incredibly diverse, we assessed the impact of Aroclor 1254 on three distinct states of in vitro polarized human macrophages: an M1 phenotype, an M2a phenotype, and an M2c phenotype. Each macrophage subset was exposed to PCBs after polarization to mimic the exposure that resident macrophages would receive during PCB accumulation in adipose tissue. To phenotype the macrophages, we assessed surface marker expression and cytokine release. We then investigated whether there is a dose- and time-dependent response to PCBs. Finally, since metabolic shifts are associated with phenotypic shifts in macrophages, we assessed whether PCB exposure results in altered macrophage cellular metabolism. The results of this work fill an important gap in knowledge about how PCB exposure contributes to immunometabolic dysfunction.

Results

PCBs enhance the inflammatory phenotype of M1 macrophages

Building on previous work showing that single-congener PCBs will polarize naïve macrophage cell lines toward an inflammatory phenotype (40–42), we first assessed how PCB exposure impacts

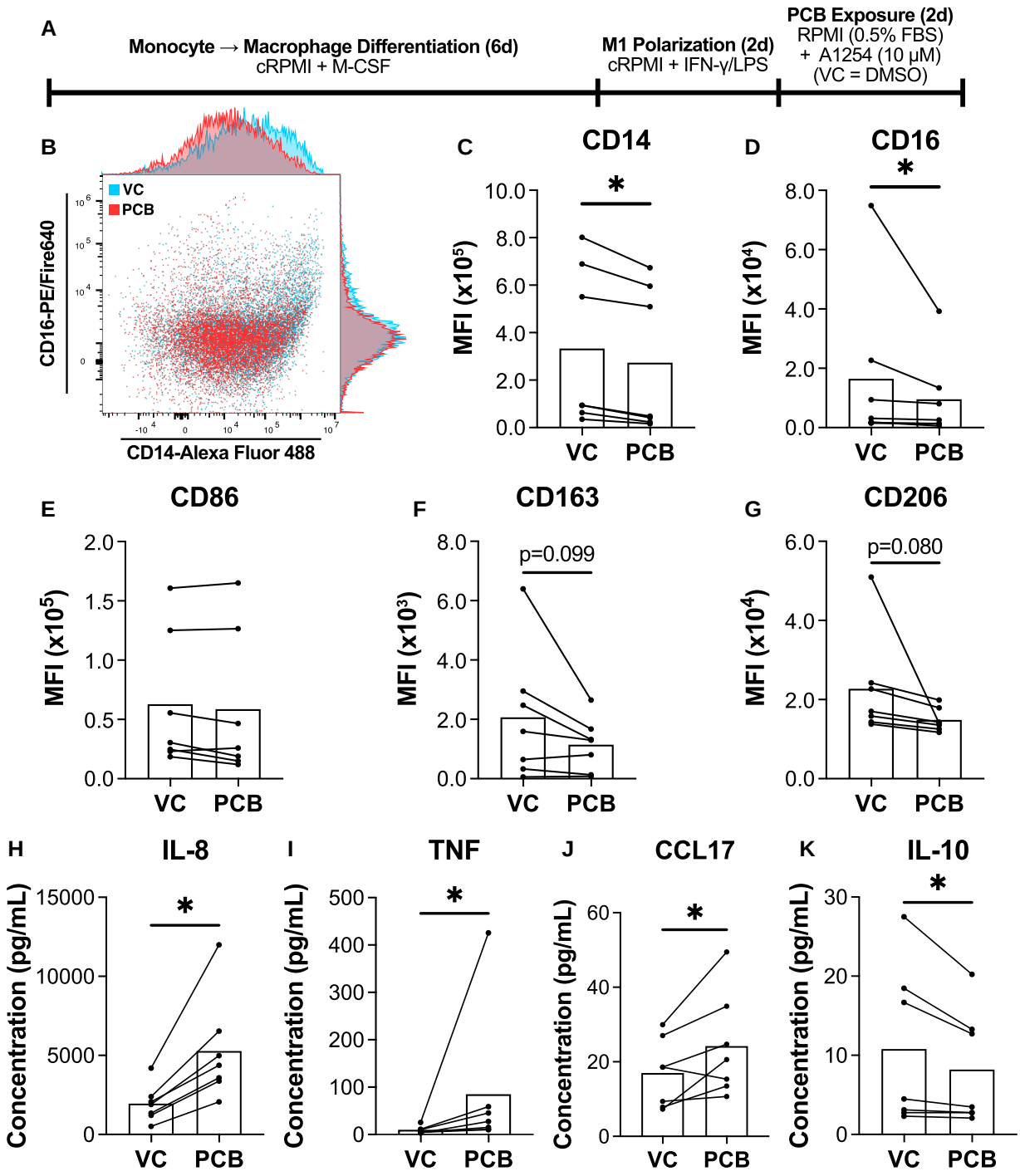

Fig. 1. PCB exposure results in increased inflammatory cytokine production, but minimal changes in surface marker expression. A) Timeline of macrophage differentiation, M1 polarization, and PCB (Aroclor 1254, 10 μM) or VC (DMSO, 0.5 μL/mL) exposure. B) Representative plot of CD14 vs. CD16 surface marker expression of vehicle-exposed (VC) and PCB-exposed (PCB) macrophages. The MFI was quantified for C) CD14, D) CD16, E) CD86, F) CD163, and G) CD206. The concentration of H) IL-8, I) TNF, J) CCL17, and K) IL-10 in culture media was measured via ELISA (IL-8, IL-10) or via a LEGENDplex bead-based multiplex assay (TNF, CCL17) (mean, $n = 7$ human donors/independent experiments; *$P < 0.05$ calculated after paired ratio t test).

inflammatory macrophages. To test our hypothesis that PCB exposure would increase the inflammatory phenotype of M1 macrophages, we exposed human monocyte-derived M1 macrophages to Aroclor 1254 for 48 h before assessing macrophage phenotype using surface marker expression and cytokine release (Fig. 1A). As a control, M1 macrophages were exposed to the vehicle, dimethyl sulfoxide (DMSO) (0.5 μL/mL), for 48 h.

M1 macrophages exposed to PCBs had minor shifts in surface marker expression compared with those only exposed to the vehicle control (VC). There was a small statistically significant downward shift in the CD14/CD16 expression upon PCB exposure (Figs. 1B–D and S1). However, PCBs did not induce statistically significant changes in CD86, an inflammatory marker (Fig. 1E), and only had minor decreases in CD163 and CD206, two antiinflammatory markers, that did not reach statistical significance (Fig. 1F and G). Even though the surface marker changes were subtle, we went on to assess functional phenotype by analyzing changes in cytokine production. Strikingly, M1 macrophages

exposed to PCBs secreted significantly more of inflammatory cytokines, IL-8 and TNF (Figs. 1H and I and S2). PCBs also increased the secretion of chemokine (C-C-motif) ligand 17 (CCL17) (Figs. 1J and S3), a chemokine implicated in obesity-associated inflammation and T cell recruitment (47–49). Corresponding to the increase in inflammatory cytokines, PCBs also decreased the amount of anti-inflammatory IL-10 secreted by the macrophages (Fig. 1K). These results indicate that Aroclor 1254 exposure enhances the inflammatory phenotype of M1 macrophages.

M2 macrophages exposed to PCBs have reduced antiinflammatory surface marker expression

During the development of adipose tissue inflammation, the resident antiinflammatory, M2 macrophages will shift toward a more inflammatory, M1-like phenotype (50). Since M2-to-M1 switching is a hallmark of metabolic disease, we wanted to assess whether PCB exposure induces phenotypic plasticity of antiinflammatory, M2 macrophages. We hypothesized that PCB-exposed M2 macrophages would shift toward a more inflammatory phenotype. To reflect the diversity of M2 subcategories found in vivo, we assessed the effect of PCB exposure on two distinct antiinflammatory macrophage phenotypes, namely M2a and M2c. To do this, we polarized five distinct donors of human monocyte-derived macrophages to an M2a or M2c state using IL-4 or dexamethasone, respectively. We then exposed them to Aroclor 1254 for 48 h before assessing surface marker phenotype (Figs. 2A and S4).

In contrast to the minimal effect PCBs had on M1 surface marker expression, surface markers on both M2a and M2c macrophages were significantly altered by PCB exposure. PCB-exposed M2a macrophages had decreased expression of both CD14 and CD16 (Fig. 2B). Furthermore, despite having little impact on the expression of inflammatory CD86, PCB exposure resulted in stark decreases in the expression of the antiinflammatory surface markers, CD163 and CD206 (Fig. 2C). Thus, M2a macrophages respond to PCB exposure by down-regulating the expression of antiinflammatory surface markers CD163 and CD206 while simultaneously maintaining the expression of inflammatory CD86 (Fig. 2D).

M2c macrophages had an even larger shift in surface marker expression in response to PCB exposure. Both CD14 and CD16 were significantly decreased (Fig. 2E). Although PCB-exposed M2c macrophages had slightly lower expression of inflammatory CD86, they had substantial 4-fold and 2-fold decreases in antiinflammatory CD163 and CD206 expression, respectively (Fig. 2F). When examined together, the decrease in CD163 and CD206 far outweighs any minor changes in CD86 again, suggesting that M2c macrophages respond to PCB exposure by preferentially down-regulating antiinflammatory surface marker expression (Fig. 2G). Notably, PCB-exposed macrophages do not have increased cell death compared with vehicle-exposed, suggesting that this is a noncytotoxic alteration in surface marker expression (Fig. S5). Overall, PCB exposure dampens the ability of both M2a and M2c macrophages to express antiinflammatory surface markers.

M2 macrophages have a dose- and time-dependent cytokine response to PCBs

To further assess how PCBs impact macrophage phenotype, we next asked whether PCB exposure impacts M2a or M2c cytokine production. To do this, we repeated the previous experiment by exposing M2a and M2c macrophages to Aroclor 1254 for 48 h. Then, we collected the media and assessed the release of IL-8 and IL-10 via enzyme-linked immunosorbent assay (ELISA). Our results show that both M2a and M2c macrophages had staggering increases in the amount of IL-8 produced—about a 400× and 1,000× increase, respectively (Figs. 3A and S5). Additionally, both M2a and M2c macrophages had significantly decreased IL-10 secretion upon exposure to PCBs (Fig. 3B). Combining these data, we see that PCB exposure results in a 5× increase in the ratio of IL-8/IL-10 in M2a macrophages and an extraordinary 60× increase for M2c macrophages (Fig. 3C). Thus, PCB exposure shifts M2 cytokine release toward a more inflammatory phenotype.

Having discovered that macrophages exposed to PCBs have a more inflammatory cytokine profile, we next wanted to know whether this response is dose-dependent. We exposed M2a and M2c macrophages to a nominal Aroclor 1254 concentration of 0, 0.1, 1, 5, 10, 20, 25, or 50 μM and then assessed secretion of IL-8 and IL-10. Upon Pearson's correlation testing, PCB concentration was strongly correlated with IL-8 secretion for both M2a ($r = 0.95$, $P < 0.01$) and M2c ($r = 0.98$, $P < 0.01$) macrophages (Fig. 4A). IL-10 production, on the contrary, had a strong negative correlation with PCB concentration for both M2a ($r = -0.95$, $P < 0.01$) and M2c ($r = -0.91$, $P < 0.01$) macrophages (Fig. 4B). Since PCBs accumulate in adipose tissue, adipose tissue macrophages are exposed to increasing concentrations of PCBs over a lifetime. Therefore, resident M2 macrophages will likely become increasingly inflammatory in response to increasing PCB concentrations.

To further simulate how PCB accumulation in adipose tissue impact macrophages, we next wanted to ask whether the magnitude of macrophage plasticity is dependent on the length of PCB exposure. Therefore, we next assessed how exposure to PCBs over 8 days, instead of 2 days, impacts macrophage cytokine release. We exposed M2a or M2c macrophages to Aroclor 1254 (10 μM) over 8 days, with media changes every 2 days. Then, we assessed the cumulative secretion of IL-8 and IL-10. Although the vehicle-exposed M2a and M2c macrophages reached a plateau of IL-8 secretion around day 4, the PCB-exposed macrophages continue to increase IL-8 secretion for all 8 days (Fig. 4C). However, the opposite occurred for IL-10. Instead, the vehicle-exposed M2a and M2c macrophages continued to secrete IL-10 for all 8 days; however, PCB-exposed macrophages stopped producing any new IL-10 by day 4 (Fig. 4D). These results show that more chronic PCB exposure, as is found in vivo, further accentuates the switch from an antiinflammatory to inflammatory phenotype.

M2a and M2c macrophages experience different metabolic shifts in response to PCB exposure

During polarization and plasticity, macrophages must undergo massive metabolic changes. To shift from an antiinflammatory, M2-like state toward a more inflammatory, M1-like state, macrophages alter their metabolism to be more greatly dependent on aerobic glycolysis and less dependent on amino acid and fatty acid oxidation (51–53). This increased dependence on glucose as a substrate allows M1 macrophages to increase flux through the pentose phosphate pathway to produce NADPH, a necessary component for scavenging reactive oxygen species (54, 55). Since our data suggest that PCBs push macrophages toward a more functionally inflammatory state, we wanted to assess whether this plasticity is accompanied by alterations in cellular metabolism.

To assess the metabolic consequences of PCB exposure, we exposed macrophages to Aroclor 1254 (10 μM) for 48 h and then used the recently developed SCENITH (Single Cell ENergetic metabolism by profiling Translation inHibition) assay to assess changes in cellular metabolism (56). The SCENITH assay provides similar insight to a Seahorse assay by using a series of metabolic inhibitors followed by quantification of protein synthesis using flow cytometry. Cells are exposed to metabolic inhibitors followed by

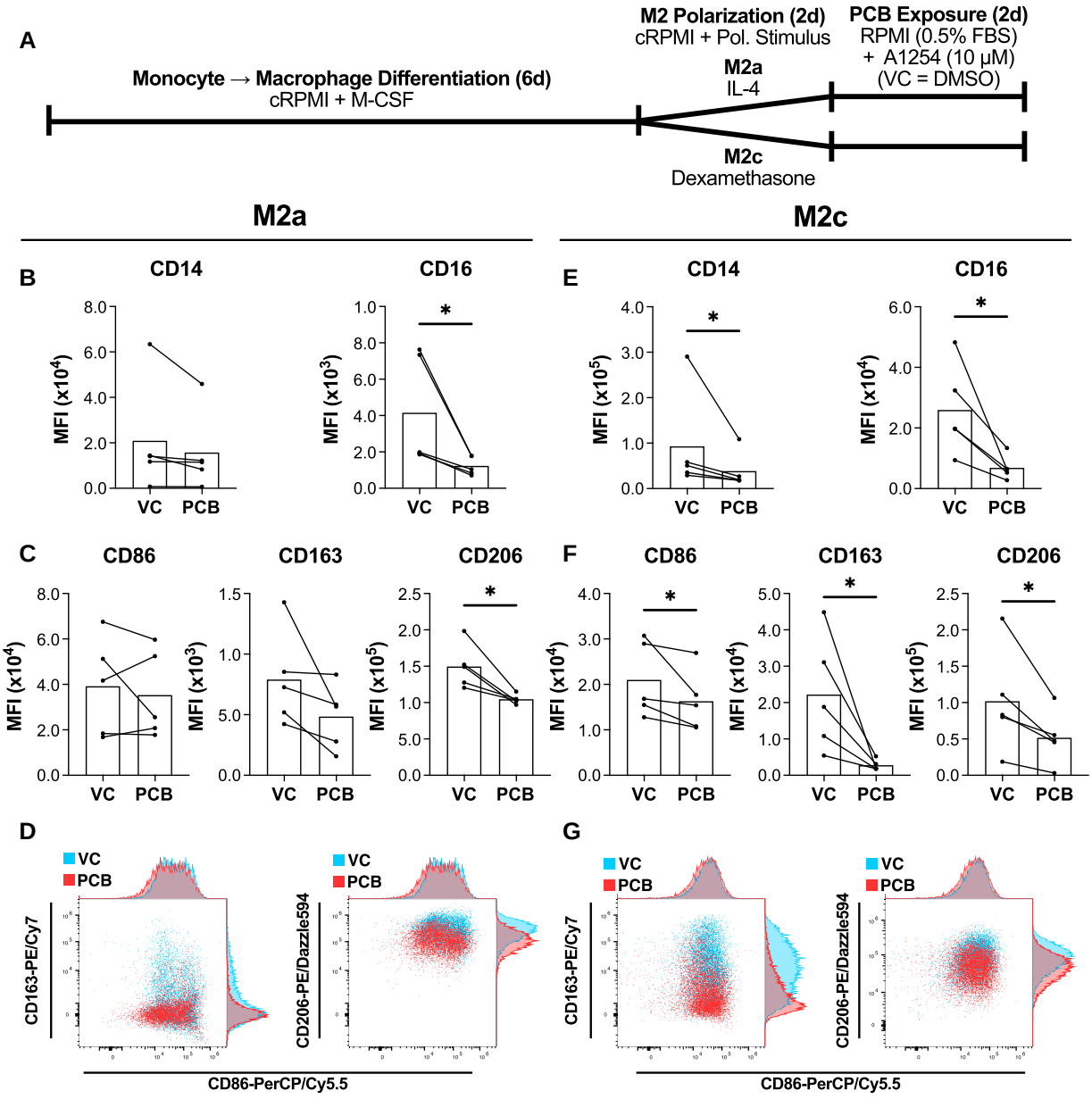

Fig. 2. PCB-exposed M2 macrophages have decreased antiinflammatory surface marker expression. A) Timeline of macrophage differentiation, M2a/M2c polarization, and PCB exposure (Aroclor 1254, 10 µM). M2a macrophages were exposed to PCBs or the vehicle (VC), DMSO, and then, surface marker expression for B) CD14 and CD16 and C) CD86, CD163, and CD206 was quantified using MFI. D) Representative plots of CD86 vs. CD163 and CD86 vs. CD206 after M2a macrophages were exposed to the vehicle (VC) or PCB (PCB). M2c macrophages were exposed to PCBs or the vehicle, DMSO (VC), and then, surface marker expression for E) CD14 and CD16 and F) CD86, CD163, and CD206 was quantified using MFI. G) Representative plots of CD86 vs. CD163 and CD86 vs. CD206 after M2c macrophages were exposed to the vehicle (VC) or PCB (PCB) (mean, $n = 5$ human donors/independent experiments; $^*P < 0.05$ calculated after paired ratio t test).

incubation with puromycin, which incorporates into newly synthesized proteins. By fixing and staining for puromycin incorporation, we can determine how much protein synthesis depends on aerobic glycolysis vs. oxidative phosphorylation.

After PCB exposure, the macrophages were incubated with either 2-deoxy-D-glucose (2-DG) to block glucose metabolism or oligomycin to inhibit oxidative phosphorylation. Additionally, macrophages treated with media alone or with the protein translation inhibitor, harringtonine, were analyzed as controls for maximum and minimum protein synthesis, respectively.

Overall, both M2a and M2c macrophages exhibited metabolic shifts associated with PCB exposure. Compared with VC-treated, PCB-exposed M2a macrophages had decreased puromycin incorporation when glucose metabolism was blocked using 2-DG and increased puromycin incorporation when oxidative phosphorylation was blocked using oligomycin (Fig. 5A). PCB-exposed M2c macrophages, on the contrary, had decreased puromycin incorporation with both 2-DG and oligomycin compared with VC-treated cells (Fig. 5B). Importantly, neither PCB exposure nor exposure to metabolic inhibitors increased macrophage cell death (Fig. S5).

To further quantify the metabolic shifts, we used the median fluorescent intensity (MFI) of puromycin incorporation to calculate the four SCENITH outputs, namely glucose dependence, mitochondrial dependence, fatty acid oxidation/amino acid oxidation (FAO/AAO) capacity, and glycolytic capacity (Fig. 5C and Tables S1 and S2). Glucose dependence and mitochondrial

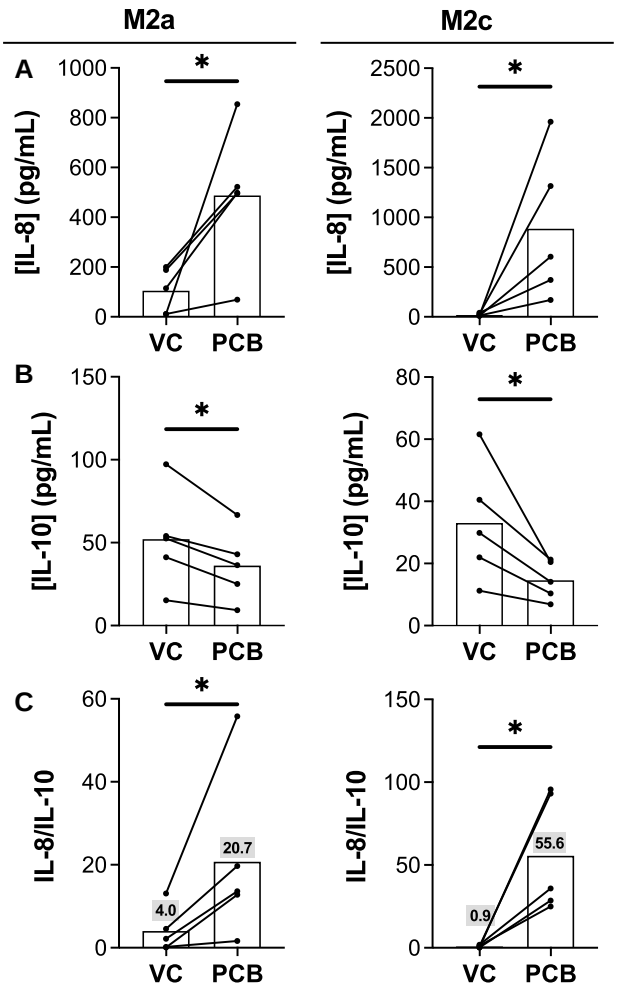

Fig. 3. PCB exposure shifts M2 macrophages toward inflamed cytokine production. M2a and M2c macrophages were exposed to a 10-μM concentration of Aroclor 1254. A) Concentration of IL-8 in culture media measured by ELISA for M2a (left) and M2c (right) macrophages. B) Concentration of IL-10 in culture media measured by ELISA for M2a (left) and M2c (right) macrophages. C) Ratio of IL-8/IL-10 (mean, $n = 5$ human donors/independent experiments; *$P < 0.05$ calculated after paired ratio t test).

dependence reflect the proportion of protein synthesis that was depleted upon incubation with 2-DG or oligomycin, respectively. But FAO/AAO capacity and glycolytic capacity reflect the ability of the cells to sustain protein synthesis using compensatory metabolic pathways when glucose metabolism or oxidative phosphorylation is blocked with 2-DG or oligomycin, respectively.

PCB-exposed M2a macrophages had increased glucose dependence and decreased FAO/AAO capacity compared with VC-treated cells (Fig. 5D). However, they did not have any change in mitochondrial dependence or glycolytic capacity (Fig. 5D). On the contrary, M2c macrophages exposed to PCBs had increased glucose dependence and mitochondrial dependence with corresponding decreases in FAO/AAO capacity and glycolytic capacity (Fig. 5E). Taken together, PCB exposure pushes both M2 macrophage subsets to become more dependent on aerobic glycolysis consistent with a shift toward a more inflammatory phenotype.

Discussion

Macrophage plasticity plays a crucial role in the development of dysfunctional adipose tissue. Healthy adipose tissue contains a macrophage niche rich in antiinflammatory macrophages. However, during the pathogenesis of diseased adipose tissue, resident macrophages are exposed to a microenvironment rich in glucose, lipids, and proinflammatory cytokines, all of which drive the macrophages to shift toward a more inflammatory phenotype (29, 57, 58). Since macrophages are so greatly influenced by the adipose microenvironment, it is imperative to understand whether toxicants that accumulate in adipose tissue, such as PCBs, alter macrophage phenotype.

Herein, we investigated whether exposure to the PCB mixture, Aroclor 1254, induces macrophage plasticity. Although Aroclor 1254 has not been manufactured for nearly 50 years, signatures of this mixture continue to be measured at high levels in water, air, food, schools, and buildings (8, 10, 11, 59–61). Due to the pervasiveness of PCB mixtures, such as Aroclor 1254, human serum, urine, and adipose samples rarely contain just one PCB congener. Rather, they contain a concoction of the many congeners found in commercially produced PCB mixtures (7, 45, 46). One of the main limitations of the previous research was that it did not reflect the complexity of human PCB exposure and was instead done using single-congener PCB exposures (40–42). To build on previous single-congener research, we sought to recapitulate exposure to an environmentally relevant mixture, Aroclor 1254. We first asked how exposure to the PCB mixture Aroclor 1254 impacts inflammatory macrophages. We showed that Aroclor 1254-exposed M1 macrophages had decreased expression of general macrophage markers, CD14 and CD16, as well as decreased expression of antiinflammatory surface markers, CD163 and CD206, although not statistically significant. More interestingly, these PCB-exposed M1 macrophages had heightened secretion of inflammatory cytokines IL-8, TNF, and CCL17 along with decreased secretion of antiinflammatory IL-10 (Fig. 1). These PCB-induced changes in the secretory profile resemble those observed in inflamed adipose tissue, with increased production of IL-8, TNF, and CCL17 all being implicated with adipose dysfunction (47, 49, 62–64). Our results also corroborate those of Wang et al. (40) and May et al. (41) who showed that exposure to PCB 126 or 118 heightens the inflammatory response to LPS stimulation. However, they are counter to those of Santoro et al. (42) who showed that exposure to PCB 101, 153, or 180 inhibits the inflammatory response. The similarities and discrepancies between our works can be explained by the chemical makeup of the congeners used. PCB congeners can be classified as either dioxin-like or nondioxin-like. Dioxin-like PCBs, such as PCB 118 and 126, are chemically similar to the highly toxic dioxin, 2,3,7,8-tetrachlorodibenzo-p-dioxin (TCDD). They exert their effects, in part, through activation of the aryl hydrocarbon receptor, whereas nondioxin-like congeners, such as PCB 101, 153, and 180, do not (65, 66). Aroclor 1254 contains an abundance of dioxin-like congeners. This is evidenced by its high dioxin toxic equivalency, which is 21, a value that provides insight into how similar a mixture is to TCDD (67). Therefore, despite also containing nondioxin-like congeners, the cumulative action of the PCBs in Aroclor 1254 mixture results in inflammation similar to that of dioxin-like congeners used by Wang et al. and May et al.

Another contribution of our work was the use of primary human macrophages polarized to both M1 and M2 phenotypes. Previous work only investigated how single-congener PCB exposure impacts naïve or M1 macrophages. However, the more interesting question in our opinion is whether PCB exposure impacts the antiinflammatory, M2 macrophages predominantly found in healthy adipose tissue. Since one of the hallmarks of diseased adipose tissue is the phenotypic switching of antiinflammatory, M2 macrophages toward a more M1-like phenotype, we assessed

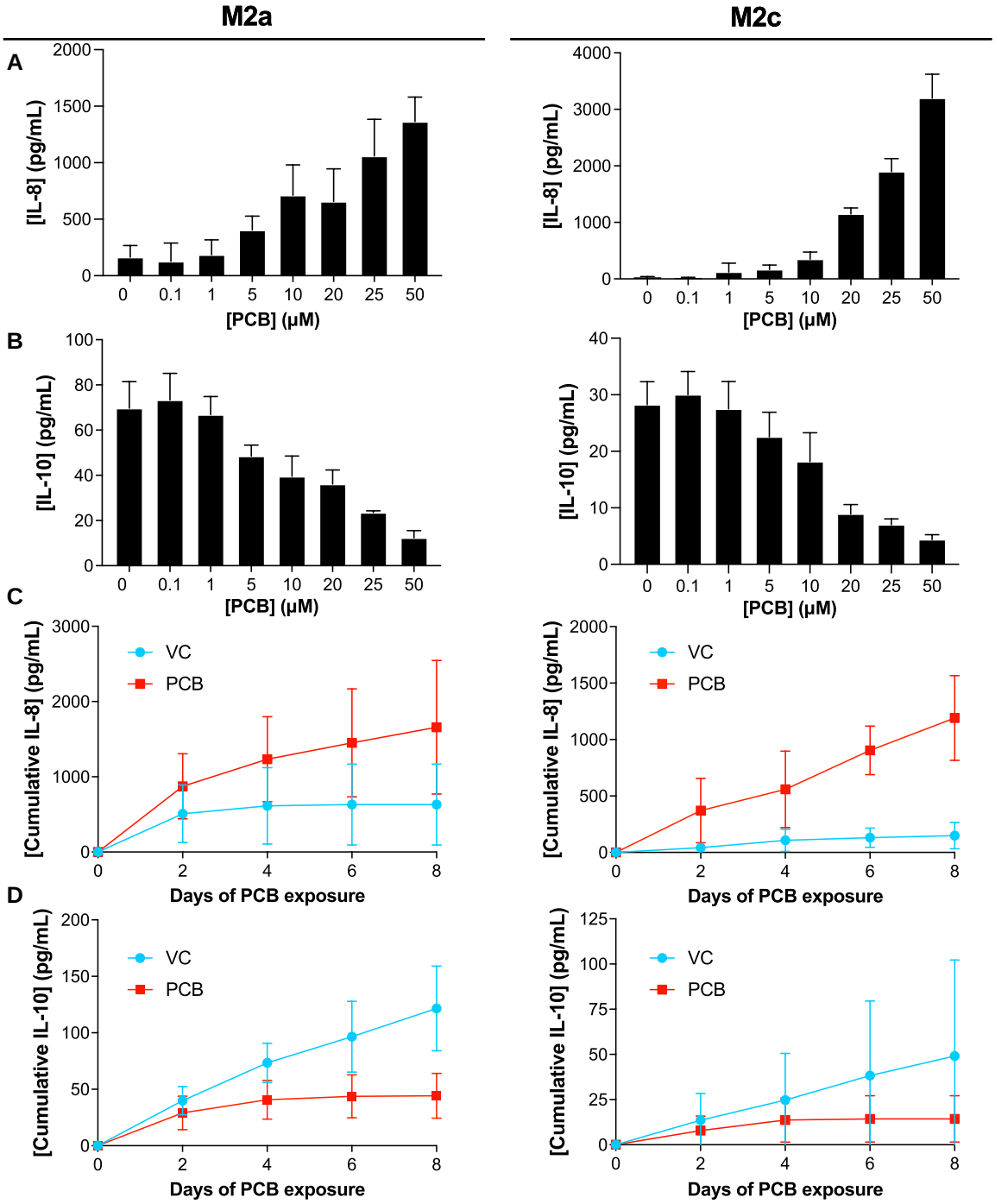

Fig. 4. M2 macrophages have a dose- and time-dependent cytokine response to PCB exposure. To test dose dependence, M2a and M2c macrophages were exposed to the 0 (VC) and 0.1, 1, 5, 10, 20, 25, or 50 μM nominal concentrations of PCBs, and then, the concentration of A) IL-8 or B) IL-10 was measured via ELISA. To test time dependence, M2a and M2c macrophages were exposed to 10 μM PCBs or the vehicle, DMSO for 2, 4, 6, or 8 days, and then, the concentration of A) IL-8 or B) IL-10 was measured (mean ± SD, $n = 3$ human donors/independent experiments).

whether exposure to Aroclor 1254 would induce macrophage plasticity. We showed that both M2a and M2c macrophages exposed to PCBs after polarization conserved expression of the inflammatory marker, CD86, while drastically decreasing the expression of antiinflammatory markers, CD163 and CD206 (Fig. 2). In adipose tissue, CD163+ macrophages work to limit iron overload due to CD163's role as a hemoglobin–haptoglobin scavenger receptor. Due to the role of iron overload in adipose tissue inflammation, loss of the CD163+ macrophages results in worsened adipose function (68). On the contrary, macrophages positive for CD206, the mannose receptor, have been shown to regulate systemic glucose by modulating adipocyte growth and differentiation (69). Thus, the selective down-regulation of antiinflammatory surface markers after PCB exposure results in a more inflammatory macrophage niche.

Macrophage biology is complex. There is overwhelming evidence to suggest that many macrophages in vivo exist as a mixed M1/M2 phenotype rather than on the extremes created by in vitro polarization. Adipose tissue alone contains a plethora of mixed phenotypes including metabolically activated macrophages,

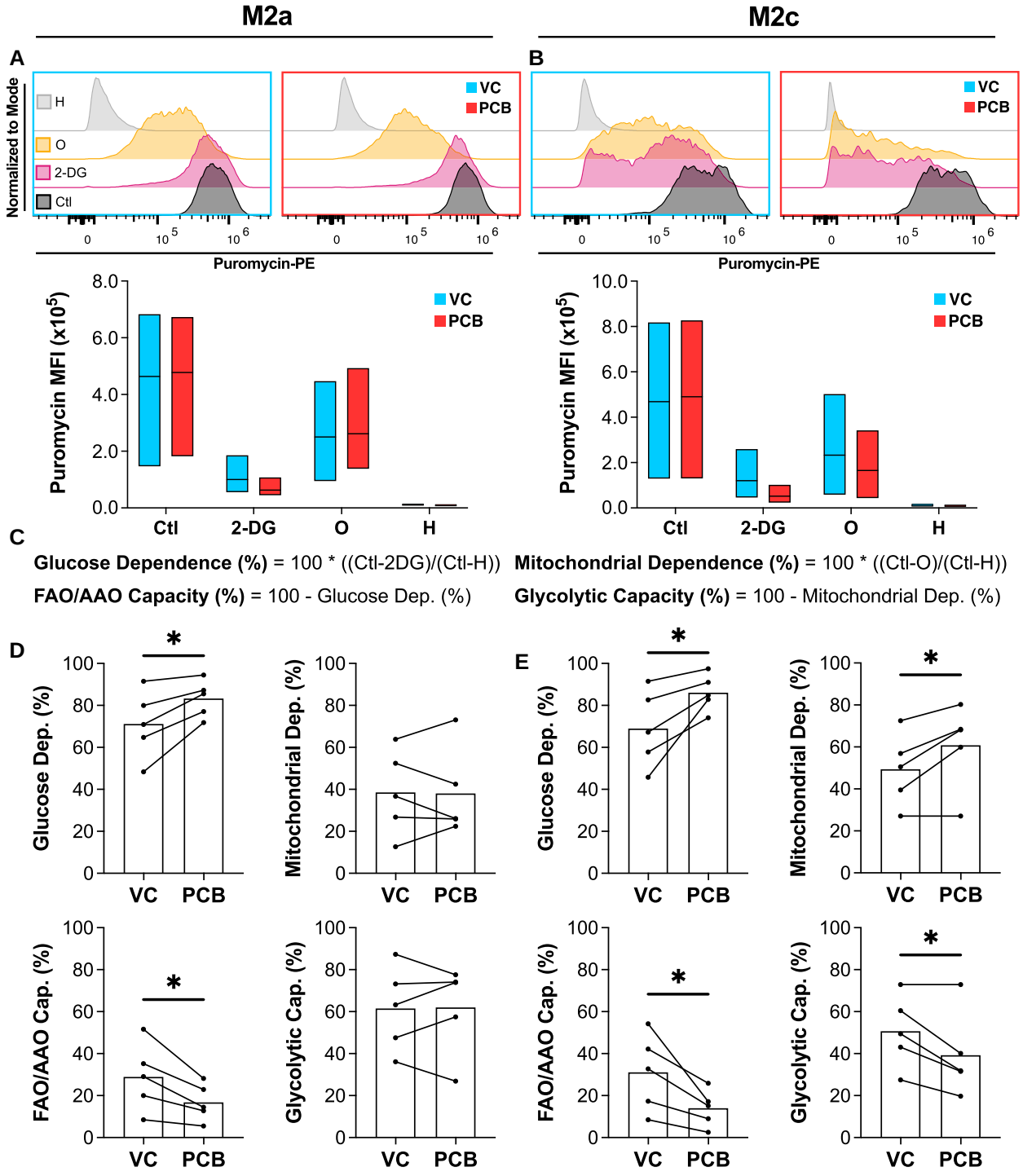

Fig. 5. PCB exposure disrupts the cellular metabolism of M2 macrophages. M2a and M2c macrophages were exposed to a 10-μM concentration of Aroclor 1254, and then, cellular metabolism was measured using the SCENITH assay. A) Representative plots for M2a puromycin incorporation and quantification of MFI after exposure to control media (Ctl), DG, oligomycin (O), and harringtonine (H). B) Representative plots for M2c puromycin incorporation and quantification of MFI. C) Equations used to calculate glucose dependence, FAO/AAO capacity, mitochondrial dependence, and glycolytic capacity. Ctl, DG, O, and H correspond to the antipuromycin MFI after exposure to control media, 2-deoxy-D-glucose, oligomycin, or harringtonine, respectively. D) Glucose dependence, FAO/AAO capacity, mitochondrial dependence, and glycolytic capacity for vehicle-exposed (VC) or PCB-exposed M2a macrophages. E) Glucose dependence, FAO/AAO capacity, mitochondrial dependence, and glycolytic capacity for vehicle-exposed (VC) or PCB-exposed M2c macrophages (mean, $n = 5$ human donors/independent experiments; *$P < 0.05$ calculated after paired t test).

lipid-associated macrophages, and crown-like structure macrophages (70). Consequently, in vivo experiments have shown that macrophage populations high in antiinflammatory surface markers, such as CD163 or CD206, are associated with insulin resistance and adipose inflammation (71–73). The ability of macrophages to undergo phenotypic plasticity is likely responsible for these mixed phenotypes. Li et al. provided evidence of this phenomenon by showing that M2 macrophages exposed to LPS did not completely repolarize to an M1-like state. Rather, these M2-to-M1 shifted macrophages maintained a mixed pro- and anti-inflammatory surface marker expression (74). However, these macrophages had other functional features providing evidence

of an inflammatory phenotype. This underscores the importance of utilizing both surface marker expression and functional readouts, such as cytokine release, to understand macrophage phenotype. Motivated by this prior work, we next assessed how PCB exposure impacts macrophage cytokine release. We found that PCB-exposed M2a and M2c macrophages had significant increases in IL-8 and decreases in IL-10 (Fig. 3). Additionally, we showed that IL-8 secretion is directly proportional to the concentration of PCB exposure, while IL-10 is inversely proportional (Fig. 4). These data further endorse our conclusion that PCB exposure induces phenotypic plasticity of M2 macrophages toward a more inflammatory phenotype.

In recent years, the field of immunometabolism has emerged to offer compelling evidence that reprogramming cellular metabolism drives macrophage phenotypic plasticity (75). It has been long known that inflammatory, M1-like macrophages will have a greater dependence on aerobic glycolysis while decreasing their dependence on fatty acids and amino acids compared with antiinflammatory, M2 phenotypes. It was originally thought that the metabolic changes are last to arrive. However, immunometabolic research has flipped this paradigm. Recent research has shown that modulation of metabolic pathways directly influences cytokine secretion and expression of inflammatory genes (76, 77). Furthermore, it is the up-regulation of glycolytic enzymes such as hexokinase and pyruvate kinase M2 (PKM2) that directly drive the activation of inflammatory transcription factors and thus the production of inflammatory cytokines (78, 79). Therefore, we hypothesized that PCB exposure would induce alterations in macrophage cellular metabolism. We showed that PCB-exposed macrophages are more greatly dependent on glucose metabolism while relying less on amino acid and fatty acid metabolism (Fig. 5). One might expect that an increase in dependence on glucose metabolism would come with a corresponding decrease in mitochondrial metabolism. However, our data show that this is not the case. M2c macrophages actually have increased dependence on both glucose and mitochondrial metabolism with PCB exposure. One possible explanation is that as PCBs shift M2c macrophages toward a more inflammatory phenotype, they cause the cells to be so greatly dependent on aerobic glycolysis and glucose as a substrate that they are pushed to maximum capacity. Consequently, when mitochondrial metabolism is blocked through oligomycin, there is no way for the cells to increase glycolysis to compensate for the lack of oxidative phosphorylation. Another possible explanation is proposed by the work of Lachmandas et al. They showed that all inflammatory stimuli will increase macrophage glycolysis; however, only those that activate TLR4 will decrease mitochondrial metabolism (80). Furthermore, there is evidence to suggest that proinflammatory adipose tissue macrophages display both increased glycolysis and oxidative phosphorylation (77).

PCB exposure has previously been shown to alter cellular metabolism in other cell types. Previous studies have shown that PCB exposure increases glycolysis (81, 82). One such paper by Zhang et al. showed that glycolysis was markedly increased with PCB exposure in HeLa cells. Furthermore, their data argue that PCB 126, 118, and 153, three congeners found in Aroclor 1254, greatly increase the expression and nuclear distribution of PKM2 (83). This increase in PKM2 has also been shown with hepatocellular carcinoma SMMC-7721 cells exposed to PCB 118 (84). PKM2 directly drives the activation of inflammatory transcription factors in macrophages. Therefore, it is possible that PCB exposure drives the up-regulation of glycolysis and PKM2 resulting in a shift toward an inflammatory phenotype. However, future work would need to be done to assess this hypothesis.

In summary, our research demonstrates that Aroclor 1254, a PCB mixture present at elevated levels in school air, significantly influences the immunometabolic plasticity of human monocyte-derived macrophages. PCB-exposed M2a and M2c macrophages have reduced antiinflammatory surface marker expression coupled with both a time- and dose-dependent increase in inflammatory cytokine release. Additionally, these PCB-exposed macrophages undergo extensive metabolic reprogramming, marked by an increased reliance on aerobic glycolysis. Collectively, these findings suggest that PCB-exposed macrophages transition toward a more M1-like state, providing a new mechanism by which PCBs contribute to metabolic disease by promoting adipose tissue inflammation.

Materials and methods

Materials

Sources of PCBs

Aroclor 1254 (lot number KC 12-638) in the original containers from Monsanto (St. Louis, MO, USA) was provided by the Synthesis Core of the ISRP.

Cell culture media

Unless otherwise specified, all cells were cultured in RPMI 1640 (Gibco, cat#: 11875093) supplemented with 1% (v/v) penicillin/streptomycin (Thermo Fisher, cat#: 15140122), 1% (v/v) L-glutamine (Thermo Fisher, cat#: 25030081), and 10% (v/v) fetal bovine serum (FBS) (VWR, cat#: 97068-085). For PCB exposure, low-serum RPMI 1640 supplemented with 0.5% (v/v) FBS was used.

Isolation of human PBMCs

Human peripheral blood mononuclear cells (PBMCs) were isolated from leukocyte reduction cones (LRC) procured through the DeGowin Blood Center at the University of Iowa. After receiving the LRC, the blood was drained and mixed with base RPMI. Then, the cell suspension was added to a LeucoSep conical tube containing Ficoll-Paque (Cytiva, cat#: 17544202) before being centrifuged for 30 min at 600 g without break. After separation, the buffy coat was collected and washed twice with 2% FBS in PBS −/−. After washing, red blood cells were lysed using 1× RBC lysis buffer (Cytek, cat#: TNB-4300-L100). The cells were then washed with complete RPMI and counted. Isolated PBMCs were then used for monocyte isolation. A total of 10 unique human donors were isolated and used for this research. The number of donors used for each experiment is noted in the figure caption.

Isolation of monocytes

After PBMC isolation, the monocytes were isolated using the MojoSort Human Pan Monocyte Isolation kit (BioLegend, cat#: 480060), a magnetic bead-based negative selection kit. The PBMCs were first washed with 1× MojoSort Buffer (1× PBS, 0.5% (w/v) BSA, and 2 mM EDTA) and filtered through a 40-μM cell strainer. Then, the cells were resuspended in 1× MojoSort Buffer to 1×10^8 PBMCs/mL. Fc receptors were blocked by incubating the cells with Human TruStain Fcx (5 μL/100 μL cell suspension) at room temperature for 10 min. Next, the negative selection Biotin-Antibody cocktail (10 μL/100 μL cell suspension) was added, and the cells were incubated on ice for 15 min. Finally, the magnetic streptavidin nanobeads were added (10 μL/100 μL cell suspension), and the cells were incubated on ice for 15 min. The cells were then washed and resuspended again in MojoSort Buffer. To isolate the monocytes, the samples were

placed in the MojoSort magnet (BioLegend, cat#: 480019) for 5 min. After 5 min, the supernatant, containing the monocytes, was collected, and the beads remaining on the walls of the tubes were resuspended in MojoSort Buffer. The magnetic separation was repeated once more to improve monocyte yield. Isolated monocytes were cryopreserved at 1×10^7 cells/mL in freezing media consisting of 50% complete RPMI, 10% DMSO, and 40% FBS. At the time of culturing, cryopreserved monocytes were thawed at 37 °C and resuspended in culture media.

Macrophage differentiation, polarization, and characterization

Monocyte-to-macrophage differentiation

All experiments were done using human monocyte-derived macrophages. To differentiate the monocytes into macrophages, the monocytes were thawed and resuspended to 1×10^6 cells/mL in media supplemented with macrophage colony stimulating factor (M-CSF) (10 ng/mL) (BioLegend, cat#: 574806). Depending on the experiment, the monocytes were plated in a 48- or 24-well plate at a cell seeding density of $\sim 4 \times 10^5$ cells/cm^2 in a volume of 750 or 434 μL/well, respectively. The cells were then differentiated to macrophages over 6 days of culturing with a media change at day 3. At day 6, the cells were considered naïve, M0 macrophages.

Macrophage polarization

Depending on the experiment, macrophages were polarized toward one of three phenotypes, M1, M2a, or M2c. To polarize toward an M1 phenotype, the macrophages were cultured in media supplemented with 50 ng/mL of IFN-γ (PeproTech, cat#: 300-02) and 25 ng/mL of LPS from *Escherichia coli* O55:B5 (Sigma-Aldrich, cat#: L6529). To polarize macrophages toward an M2a phenotype, they were cultured in media supplemented with 20 ng/mL IL-4 (PeproTech, cat#: 200-04) for 48 h. To polarize macrophages toward an M2c phenotype, they were cultured in media supplemented with 100 nM dexamethasone (Sigma-Aldrich, cat#: D4902) for 48 h. To confirm macrophage polarization was successful, surface marker expression of CD14, CD16, CD86, CD163, and CD206 for M0, M1, M2a, and M2c VC-exposed macrophage was compiled (Fig. S7) and found to be consistent with previous reports (85).

PCB exposure

At the time of PCB exposure, the macrophage polarization media were removed, and the cells were washed with 1× PBS−/− to remove residual media. All PCB exposure was done using a low-serum media RPMI 1640. Unless otherwise specified, the media were then supplemented with Aroclor 1254 at a nominal concentration of 10 μM, or the vehicle, DMSO. After 48 h of PCB exposure, the cells and/or media were collected for further analysis.

Surface marker expression

Macrophage surface markers were analyzed using flow cytometry. Briefly, the macrophages were lifted using 5 mM EDTA in PBS on ice to prevent cleavage of surface markers of interest (86). Once collected, the macrophages were stained for viability using Zombie B550 Fixable Viability Kit (BioLegend, cat#: 423122). Then, nonspecific binding was blocked using True-Stain Monocyte Blocker (BioLegend, cat#: 426103) and Human TruStain FcX (BioLegend, cat#: 422302). Then, the cells were stained with the following antihuman antibodies: CD14-Alexa Fluor 488 (BioLegend, cat#: 325610), CD16-PE-Fire 640 (BioLegend, cat#: 302068), CD86-PerCP-Cy5.5 (BioLegend, cat#: 374216), CD163-PE-Cy7 (BioLegend, cat#: 333614), and CD206-PE-Dazzle (BioLegend, cat#: 321130). After staining, the cells were washed and resuspended in Cell Staining Buffer (BioLegend, cat#: 420201).

The flow cytometry data were collected using a Cytek Northern Lights spectral cytometer equipped with a 488-nm laser and 14 fluorescent emission filters. Before the collection of experimental data, instrument and gate settings were prepared using unstained cells as a negative control or single-color stained macrophages with known surface marker expression (M1 for CD86, M2a for CD206, and M2c for CD163) as a positive control. The experimental data were assessed using FlowJo (BD Sciences). Cells were gated based on singlet discrimination (SSC-A/SSC-H and FSC-A/FSC-H) and viability (negative Zombie B550 stain). Then, surface marker expression was quantified using the MFI (Fig. S8). A total of 5–7 experiments were done with monocyte-derived macrophages from separate human donors. For each donor, each experimental condition was performed in triplicate, and the mean of the triplicate was then used as a single data point to represent the average for that donor in Figs. 1 and 2 (Figs. S1 and S3).

Cytokine release and metabolic profiling

Enzyme-linked immunosorbent assay

The concentration of IL-8 and IL-10 was analyzed using ELISAs (IL-8: BioLegend, cat#: 431504 and IL-10: BioLegend, cat#: 430604). To perform the assay, media were collected at the end of each experiment and stored at −20 °C until analysis. For analysis, the protocol was followed as described by BioLegend. Absorbance was read at 450 nm on a plate reader. Nonspecific background was subtracted from each well by reading the plate at 570 nm. A standard curve of known IL-8 or IL-10 concentrations was used as a positive control, and ELISA diluent alone was used as a negative control. A total of 5–7 experiments were done with monocyte-derived macrophages from separate human donors. For each donor, each experimental condition was performed in triplicate wells, and the mean of the triplicate was used as a single data point representing the average for that donor in Figs. 1 and 2 (Fig. S6).

LEGENDplex panel

The concentration of TNF and CCL17 was analyzed using a LEGENDplex Human Macrophage/Microglia Panel (BioLegend, cat#: 740502). To perform the assay, media were collected at the end of each experiment and stored at −20 °C until analysis. Since triplicate data from plate-based ELISAs had been highly consistent, we used physical averaging to reduce the cost of the multiplex panel. To physically average triplicate wells for each donor, equal parts media from each well were mixed prior to performing the LEGENDplex assay. Then, the protocol was followed as described by BioLegend. A standard curve of known concentrations was used as a positive control, and assay diluent alone was used as the negative control. Around 500 capture beads per target analyte were analyzed for each sample via flow cytometry before the data were processed using Qognit Data Analysis Software Suite for LEGENDplex (BioLegend) (Fig. S3). In addition to TNF and CCL17, the panel measured IL-12p70, IL-6, IL-4, IL-1β, arginase, IL-1RA, IL-10, IL-12p40, IL-23, IFN-γ, and IP-10 (Fig. S2).

SCENITH

The SCENITH protocol was performed as previously described (56, 87). This assay measures cellular energy metabolism by exposing cells to an array of metabolic inhibitors and then measuring

protein synthesis using puromycin incorporation. For a given experimental replicate, a total of four wells were used, one for each inhibitor/control. At the time of data collection, the media were removed and macrophages were washed once with cold PBS. Then, 2-DG (100 mM), oligomycin (1 μM), the negative control, harringtonine (2 μg/mL), or the positive control, complete RPMI were added to respective wells to inhibit metabolic pathways. After 20 min of incubation at 37 °C, puromycin (10 μg/mL) was added to each well. The cells were incubated at 37 °C for 30–45 min, after which the inhibitors such as puromycin were removed and the cells were washed once with cold PBS. Then, the macrophages were lifted using 5 mM EDTA in PBS. After lifting, the cells were washed again with cold PBS and stained using the live/dead Zombie B550 Fixable Viability Kit (BioLegend, cat#: 423122). During live/dead staining, the macrophage Fc receptors were blocked using Human TruStain FcX (BioLegend, cat#: 422302). After 15 min of staining and Fc blocking at room temperature, the macrophages were washed with PBS and fixed using FluoroFix Buffer (BioLegend, cat#: 422101). After 30 min of fixation, the cells were permeabilized using Intracellular Staining Permeabilization Wash Buffer (BioLegend, cat#: 421002). After permeabilization, the cells were stained with PE antipuromycin antibody (BioLegend, cat#: 381504) for an hour at 4 °C. The samples were then washed twice and analyzed by flow cytometry.

The flow cytometry data were analyzed using FlowJo (BD Sciences). First, the cells were gated for singlet discrimination using SSC-A/SSC-H and FSC-A/FSC-H. Then, each condition was gated by selecting the negative Zombie B550 population. Finally, we set a harringtonine baseline gate. Then, we assessed the fluorescence intensity of PE antipuromycin using MFI (Fig. S9). A total of five experiments were done with monocyte-derived macrophages from five separate human donors. Each experiment's VC/PCB exposure condition was performed in triplicate wells, and the mean of the triplicate was used as a single data point in Fig. 5 to describe the average for each donor.

Data analysis

All statistical analysis and graphing were performed using GraphPad Prism 10. All t tests were paired by donor. A *P*-value of < 0.05 was considered statistically significant. Further statistical details are provided within each figure caption.

Acknowledgments

The authors thank Dr Hans-Joachim Lehmler and Dr Xueshu Li, Synthesis Core, ISRP, for providing stocks of Aroclor 1254. The authors also acknowledge the University of Iowa Tissue Procurement Core which manages the University of Iowa Biobank (IRB#201103721) for services provided related to the acquisition of study specimens.

Supplementary Material

Supplementary material is available at *PNAS Nexus* online.

Funding

This study was supported by the NIEHS P42ES013661 (J.A.A. and A.J.K.). R.M.B.-.B was supported by the NIGMS T32GM139776, and NIEHS F30ES035622. The TPC was supported by NCI P30CA086862 and the University of Iowa Carver College of Medicine.

Author Contributions

J.A.A. was involved in conceptualization, resources, formal analysis, supervision, funding acquisition, investigation, methodology, project administration, and writing—review and editing. R.M.B.-.B. was involved in conceptualization, formal analysis, investigation, visualization, methodology, writing—original draft, and writing—review and editing. M.V.S. was involved in formal analysis, methodology, and writing—review and editing. E.K. was involved in formal analysis, investigation, and writing—review and editing. J.N.L was involved in formal analysis, investigation, methodology, and writing—review and editing. L.M.B. and K.E. were involved in resources, methodology, and writing—review and editing. A.J.K. was involved in conceptualization, funding acquisition, project administration, and writing—review and editing.

Data Availability

All study data are included in the article and/or supporting information.

References

1 Hornbuckle KC. 2022. Common misconceptions about PCBs obscure the crisis of Children's exposure in school. *Environ Sci Technol*. 56:16544–16545.
2 Herrick RF, McClean MD, Meeker JD, Baxter LK, Weymouth GA. 2004. An unrecognized source of PCB contamination in schools and other buildings. *Environ Health Persp*. 112:1051–1053.
3 Gore AC, *et al*. 2015. EDC-2: the Endocrine Society's second scientific statement on endocrine-disrupting chemicals. *Endocr Rev*. 36:E1–E150.
4 Mayes BA, *et al*. 1998. Comparative carcinogenicity in Sprague-Dawley rats of the polychlorinated biphenyl mixtures Aroclors 1016, 1242, 1254, and 1260. *Toxicol Sci*. 41:62–76.
5 Erickson MD, Kaley RG. 2011. Applications of polychlorinated biphenyls. *Environ Sci Pollut R*. 18:135–151.
6 Saktrakulkla P, *et al*. 2020. Polychlorinated biphenyls in food. *Environ Sci Technol*. 54:11443–11452.
7 Ampleman MD, *et al*. 2015. Inhalation and dietary exposure to PCBs in urban and rural cohorts via congener-specific measurements. *Environ Sci Technol*. 49:1156–1164.
8 Marek RF, Thorne PS, Herkert NJ, Awad AM, Hornbuckle KC. 2017. Airborne PCBs and OH-PCBs inside and outside urban and rural U.S. schools. *Environ Sci Technol*. 51:7853–7860.
9 Liebl B, *et al*. 2004. Evidence for increased internal exposure to lower chlorinated polychlorinated biphenyls (PCB) in pupils attending a contaminated school. *Int J Hyg Envir Heal*. 207:315–324.
10 Hua JBX, Marek RF, Hornbuckle KC. 2023. Polyurethane foam emission samplers to identify sources of airborne polychlorinated biphenyls from glass-block windows and other room surfaces in a Vermont school. *Environ Sci Technol*. 57:14310–14318.
11 Bannavti MK, Jahnke JC, Marek RF, Just CL, Hornbuckle KC. 2021. Room-to-room variability of airborne polychlorinated biphenyls in schools and the application of air sampling for targeted source evaluation. *Environ Sci Technol*. 55:9460–9468.
12 Everett CJ, Frithsen I, Player M. 2010. Relationship of polychlorinated biphenyls with type 2 diabetes and hypertension. *J Environ Monitor*. 13:241–251.
13 Silverstone AE, *et al*. 2012. Polychlorinated biphenyl (PCB) exposure and diabetes: results from the Anniston Community Health Survey. *Environ Health Persp*. 120:727–732.

14 Thayer KA, Heindel JJ, Bucher JR, Gallo MA. 2012. Role of environmental chemicals in diabetes and obesity: a national toxicology program workshop review. *Environ Health Persp*. 120:779–789.
15 Montano L, *et al*. 2022. Polychlorinated biphenyls (PCBs) in the environment. *Occupational and Exposure Events, Effects on Human Health and Fertility*. *Toxics*. 10:365.
16 Huang PL. 2009. A comprehensive definition for metabolic syndrome. *Dis Model Mech*. 2:231–237.
17 Kahn CR, Wang G, Lee KY. 2019. Altered adipose tissue and adipocyte function in the pathogenesis of metabolic syndrome. *J Clin Invest*. 129:3990–4000.
18 Regnier SM, Sargis RM. 2014. Adipocytes under assault: environmental disruption of adipose physiology. *Biochim Biophys Acta*. 1842:520–533.
19 Wang H, *et al*. 2020. Comprehensive subchronic inhalation toxicity assessment of an indoor school air mixture of PCBs. *Environ Sci Technol*. 54:15976–15985.
20 Wang H, Adamcakova-Dodd A, Lehmler H-J, Hornbuckle KC, Thorne PS. 2021. Toxicity assessment of 91-day repeated inhalation exposure to an indoor school air mixture of PCBs. *Environ Sci Technol*. 56(3).
21 Klingelhutz AJ, *et al*. 2018. Scaffold-free generation of uniform adipose spheroids for metabolism research and drug discovery. *Sci Rep-UK*. 8:523.
22 Behan-Bush RM, *et al*. 2022. Toxicity impacts on human adipose MSCs acutely exposed to Aroclor and non-Aroclor mixtures of PCBs. *Environ Sci Technol*. 57(4):1731–1742.
23 Gourronc FA, *et al*. 2022. Transcriptome sequencing of 3,3′,4,4′,5-pentachlorobiphenyl (PCB126)-treated human preadipocytes demonstrates progressive changes in pathways associated with inflammation and diabetes. *Toxicol In Vitro*. 83:105396.
24 Crewe C, An YA, Scherer PE. 2017. The ominous triad of adipose tissue dysfunction: inflammation, fibrosis, and impaired angiogenesis. *J Clin Invest*. 127:74–82.
25 Catrysse L, van Loo G. 2018. Adipose tissue macrophages and their polarization in health and obesity. *Cell Immunol*. 330: 114–119.
26 Mosser DM, Edwards JP. 2008. Exploring the full spectrum of macrophage activation. *Nat Rev Immunol*. 8:958–969.
27 Murray PJ, *et al*. 2014. Macrophage activation and polarization: nomenclature and experimental guidelines. *Immunity*. 41:14–20.
28 Pan D, Li G, Jiang C, Hu J, Hu X. 2023. Regulatory mechanisms of macrophage polarization in adipose tissue. *Front Immunol*. 14: 1149366.
29 Thomas D, Apovian C. 2017. Macrophage functions in lean and obese adipose tissue. *Metabolis*. 72:120–143.
30 Xu H, *et al*. 2003. Chronic inflammation in fat plays a crucial role in the development of obesity-related insulin resistance. *J Clin Invest*. 112:1821–1830.
31 Hotamisligil GS. 2006. Inflammation and metabolic disorders. *Nature*. 444:860–867.
32 Schipper HS, Prakken B, Kalkhoven E, Boes M. 2012. Adipose tissue-resident immune cells: key players in immunometabolism. *Trends Endocrinol Metabolism*. 23:407–415.
33 Zhang S, *et al*. 2015. Chronic exposure to Aroclor 1254 disrupts glucose homeostasis in male mice via inhibition of the insulin receptor signal pathway. *Environ Sci Technol*. 49:10084–10092.
34 Petriello MC, *et al*. 2017. Dioxin-like PCB 126 increases systemic inflammation and accelerates atherosclerosis in lean LDL receptor-deficient mice. *Toxicol Sci*. 162:548–558.
35 Arsenescu V, Arsenescu RI, King V, Swanson H, Cassis LA. 2008. Polychlorinated biphenyl-77 induces adipocyte differentiation and proinflammatory adipokines and promotes obesity and atherosclerosis. *Environ Health Persp*. 116:761–768.
36 Baker NA, *et al*. 2013. Coplanar polychlorinated biphenyls impair glucose homeostasis in lean C57BL/6 mice and mitigate beneficial effects of weight loss on glucose homeostasis in obese mice. *Environ Health Persp*. 121:105–110.
37 Baker NA, *et al*. 2015. Effects of adipocyte aryl hydrocarbon receptor deficiency on PCB-induced disruption of glucose homeostasis in lean and obese mice. *Environ Health Persp*. 123:944–950.
38 Kim MJ, *et al*. 2012. Inflammatory pathway genes belong to major targets of persistent organic pollutants in adipose cells. *Environ Health Persp*. 120:508–514.
39 Rolle-Kampczyk U, *et al*. 2020. Accumulation of distinct persistent organic pollutants is associated with adipose tissue inflammation. *Sci Total Environ*. 748:142458.
40 Wang C, Petriello MC, Zhu B, Hennig B. 2019. PCB 126 induces monocyte/macrophage polarization and inflammation through AhR and NF-κB pathways. *Toxicol Appl Pharm*. 367:71–81.
41 May P, *et al*. 2018. In vitro cocktail effects of PCB-DL (PCB118) and bulky PCB (PCB153) with BaP on adipogenesis and on expression of genes involved in the establishment of a pro-inflammatory state. *Int J Mol Sci*. 19:841.
42 Santoro A, *et al*. 2015. Polychlorinated biphenyls (PCB 101, 153, and 180) impair murine macrophage responsiveness to lipopolysaccharide: involvement of NF-κB pathway. *Toxicol Sci*. 147: 255–269.
43 Andreu N, *et al*. 2017. Primary macrophages and J774 cells respond differently to infection with Mycobacterium tuberculosis. *Sci Rep*. 7:42225.
44 Hoppenbrouwers T, *et al*. 2022. Functional differences between primary monocyte-derived and THP-1 macrophages and their response to LCPUFAs. *PharmaNutrition*. 22:100322.
45 Marek RF, Thorne PS, Wang K, DeWall J, Hornbuckle KC. 2013. PCBs and OH-PCBs in serum from children and mothers in urban and rural U.S. communities. *Environ Sci Technol*. 47:3353–3361.
46 Fernandez MF, *et al*. 2008. Polychlorinated biphenyls (PCBs) and hydroxy-PCBs in adipose tissue of women in Southeast Spain. *Chemosphere*. 71:1196–1205.
47 Hueso L, *et al*. 2023. CCL17 and CCL22 chemokines are upregulated in human obesity and play a role in vascular dysfunction. *Front. Endocrinol*. 14:1154158.
48 AL-Ayadhi LY, Mostafa GA. 2013. Elevated serum levels of macrophage-derived chemokine and thymus and activation-regulated chemokine in autistic children. *J Neuroinflammation*. 10:846.
49 Lee KM-C, *et al*. 2025. Therapeutic blockade of CCL17 in obesity-exacerbated osteoarthritic pain and disease. *PLoS One*. 20:e0317399.
50 Lumeng CN, Bodzin JL, Saltiel AR. 2007. Obesity induces a phenotypic switch in adipose tissue macrophage polarization. *J Clin Invest*. 117:175–184.
51 Heiden MGV, Cantley LC, Thompson CB. 2009. Understanding the Warburg effect: the metabolic requirements of cell proliferation. *Science*. 324:1029–1033.
52 Adamik J, *et al*. 2022. Distinct metabolic states guide maturation of inflammatory and tolerogenic dendritic cells. *Nat Commun*. 13: 5184.
53 Liu Y, *et al*. 2021. Metabolic reprogramming in macrophage responses. *Biomark Res*. 9:1.
54 Baardman J, *et al*. 2018. A defective pentose phosphate pathway reduces inflammatory macrophage responses during hypercholesterolemia. *Cell Rep*. 25:2044–2052.e5.

55 Sun X, *et al.* 2022. Macrophage polarization, metabolic reprogramming, and inflammatory effects in ischemic heart disease. *Front Immunol.* 13:934040.

56 Argüello RJ, *et al.* 2020. SCENITH: a flow cytometry-based method to functionally profile energy metabolism with single-cell resolution. *Cell Metab.* 32:1063–1075.e7.

57 Yao J, Wu D, Qiu Y. 2022. Adipose tissue macrophage in obesity-associated metabolic diseases. *Front Immunol.* 13:977485.

58 Ruggiero AD, Key C-CC, Kavanagh K. 2021. Adipose tissue macrophage polarization in healthy and unhealthy obesity. *Front Nutr.* 8:625331.

59 Bannavti MK, Marek RF, Just CL, Hornbuckle KC. 2023. Congener-specific emissions from floors and walls characterize indoor airborne polychlorinated biphenyls. *Environ Sci Technol Lett.* 10:762–767.

60 Martinez A, Hua JBX, Haque E, Hornbuckle KC, Thorne PS. 2022. Occurrence and spatial distribution of individual polychlorinated biphenyl congeners in residential soils from East Chicago, southwest Lake Michigan. *Sci Total Environ.* 850:157705.

61 Jahnke JC, Martinez A, Hornbuckle KC. 2022. Distinguishing Aroclor and non-Aroclor sources to Chicago Air. *Sci Total Environ.* 823:153263.

62 Kim C-S, *et al.* 2006. Circulating levels of MCP-1 and IL-8 are elevated in human obese subjects and associated with obesity-related parameters. *Int J Obes.* 30:1347–1355.

63 Bruun JM, *et al.* 2004. Higher production of IL-8 in visceral vs. subcutaneous adipose tissue. Implication of nonadipose cells in adipose tissue. *Am J Physiol Endocrinol Metab.* 286:E8–E13.

64 Hotamisligil GS, Arner P, Caro JF, Atkinson RL, Spiegelman BM. 1995. Increased adipose tissue expression of tumor necrosis factor-alpha in human obesity and insulin resistance. *J Clin Invest.* 95:2409–2415.

65 Zhang W, *et al.* 2012. PCB 126 and other dioxin-like PCBs specifically suppress hepatic PEPCK expression via the aryl hydrocarbon receptor. *PLoS One.* 7:e37103.

66 Baars AJ, *et al.* 2004. Dioxins, dioxin-like PCBs and non-dioxin-like PCBs in foodstuffs: occurrence and dietary intake in The Netherlands. *Toxicol Lett.* 151:51–61.

67 Rushneck DR, *et al.* 2004. Concentrations of dioxin-like PCB congeners in unweathered Aroclors by HRGC/HRMS using EPA method 1668A. *Chemosphere.* 54:79–87.

68 Ameka MK, *et al.* 2022. An iron refractory phenotype in obese adipose tissue macrophages leads to adipocyte iron overload. *Int J Mol Sci.* 23:7417.

69 Nawaz A, *et al.* 2017. CD206+ M2-like macrophages regulate systemic glucose metabolism by inhibiting proliferation of adipocyte progenitors. *Nat Commun.* 8:286.

70 Chavakis T, Alexaki VI, Ferrante AW. 2023. Macrophage function in adipose tissue homeostasis and metabolic inflammation. *Nat Immunol.* 24:757–766.

71 Jia Q, Morgan-Bathke ME, Jensen MD. 2020. Adipose tissue macrophage burden, systemic inflammation, and insulin resistance. *Am J Physiol Endocrinol Metab.* 319:E254–E264.

72 Muir LA, *et al.* 2022. Human CD206 + macrophages associate with diabetes and adipose tissue lymphoid clusters. *JCI Insight.* 7: e146563.

73 Sindhu S, Thomas R. 2015 (2015). Changes in the adipose tissue expression of CD86 costimulatory ligand and CD163 scavenger receptor in obesity and type-2 diabetes: implication for metabolic disease. *J. Glycom. Lipidom.* 05.

74 Li Y, *et al.* 2020. Imaging of macrophage mitochondria dynamics in vivo reveals cellular activation phenotype for diagnosis. *Theranostics.* 10:2897–2917.

75 den Bossche JV, O'Neill LA, Menon D. 2017. Macrophage immunometabolism: where are we (going)? *Trends Immunol.* 38: 395–406.

76 Thibaut R, Orliaguet L, Ejlalmanesh T, Venteclef N, AlzaidF. 2022. Perspective on direction of control: cellular metabolism and macrophage polarization. *Front Immunol.* 13:918747.

77 Boutens L, *et al.* 2018. Unique metabolic activation of adipose tissue macrophages in obesity promotes inflammatory responses. *Diabetologia.* 61:942–953.

78 Palsson-McDermott EM, *et al.* 2015. Pyruvate kinase M2 regulates Hif-1α activity and IL-1β induction and is a critical determinant of the Warburg effect in LPS-activated macrophages. *Cell Metab.* 21: 65–80.

79 Jesus AD, *et al.* 2022. Hexokinase 1 cellular localization regulates the metabolic fate of glucose. *Mol Cell.* 82:1261–1277.e9.

80 Lachmandas E, *et al.* 2016. Microbial stimulation of different toll-like receptor signalling pathways induces diverse metabolic programmes in human monocytes. *Nat Microbiol.* 2: 16246.

81 Qin Q, Yang B, Liu J, Song E, Song Y. 2022. Polychlorinated biphenyl quinone exposure promotes breast cancer aerobic glycolysis: an in vitro and in vivo examination. *J Hazard Mater.* 424: 127512.

82 McCann MS, Fernandez HR, Flowers SA, Maguire-Zeiss KA. 2021. Polychlorinated biphenyls induce oxidative stress and metabolic responses in astrocytes. *Neurotoxicology.* 86:59–68.

83 Zhang Y, Song L, Li Z. 2019. Polychlorinated biphenyls promote cell survival through pyruvate kinase M2-dependent glycolysis in HeLa cells. *Toxicol Mech Methods.* 29:428–437.

84 Liang W, Zhang Y, Song L, Li Z. 2019. 2,3′4,4′,5-Pentachlorobiphenyl induces hepatocellular carcinoma cell proliferation through pyruvate kinase M2-dependent glycolysis. *Toxicol Lett.* 313:108–119.

85 Purcu DU, *et al.* 2022. Effect of stimulation time on the expression of human macrophage polarization markers. *PLoS One.* 17: e0265196.

86 Chen S, So EC, Strome SE, Zhang X. 2015. Impact of detachment methods on M2 macrophage phenotype and function. *J Immunol Methods.* 426:56–61.

87 Verberk SGS, *et al.* 2022. An integrated toolbox to profile macrophage immunometabolism. *Cell Rep Methods.* 2:100192.